ELSEVIER

Journal of Alloys and Compounds 235 (1996) 256–261

Journal of ALLOYS AND COMPOUNDS

Phase equilibria in the Mn-rich portion of the binary system Mn–Al

X.J. Liu, R. Kainuma, H. Ohtani, K. Ishida*

Department of Materials Science, Faculty of Engineering, Tohoku University, Sendai 980-77, Japan

Received 9 October 1995

Abstract

The phase equilibria in the binary Mn–Al system have been investigated over the temperature range 800 to 1200 °C and the composition range 50 to 80 at.% Mn using a combination of diffusion couple techniques, optical metallography, X-ray diffraction, and differential scanning calorimetry. The results show that: (i) the ε/δ – Mn phase boundary is located at approximately 72 at.% Mn, (ii) the ε phase region is wider and extends to higher Mn content than that reported before, and (iii) the eutectoid reaction (δ-Mn $\rightarrow \varepsilon + \beta$-Mn) occurs at approximately 1040 °C, i.e. at a temperature higher than that previously reported (970 °C). While the results from this study on the ε/γ and ε/β-Mn phase equilibria are in satisfactory agreement with the data of previous workers, the results on the ε/δ-Mn phase equilibrium differ from those reported previously. It is explained that this discrepancy may be due to the presence of the previously undetected transformation from the ε to the β-Mn phase on quenching, which occurs only in the ε phase alloys with Mn content over 58 at.%.

Keywords: Phase equilibria; Phase transformation; Magnetic alloy; Diffusion couple; Mn–Al phase diagram

1. Introduction

The technological importance of phase equilibria studies in the binary system Mn–Al arises from the fact that the ferromagnetic metastable τ phase in the Mn–Al binary system is of great interest as a material for permanent magnets because of its high magnetic anisotropy. This phase occurs when the high temperature ε (cph) phase transforms to a metastable τ ($L1_0$) phase during cooling from the ε phase region at rates higher than 10 °C s^{-1} [1,2], or during tempering of retained ε phase at lower temperatures [3,4]. The general form of the Mn–Al phase diagram was established in the 1940s using mainly DTA techniques [5]. Some further investigations based on magnetic measurements, microscopy, specific heat and structure analysis, resulted in a modified phase diagram [1–3,6–8]. Later, in 1987, McAlister and Murray [9] assessed the Mn–Al phase diagram. The crystal structure of the high temperature γ phase was then unknown, because this phase could not be retained by quenching [9]. However, Ellner [10] has recently found that the γ phase is isotypic with tungsten, and has a lattice parameter $a = 0.3063$ nm, as determined by high temperature X-ray diffraction. More recently, thermodynamic calculations pertaining to phase equilibria in this system have been carried out by Jansson [11]. The Mn-rich part of the most recent version of this system is redrawn in Fig. 1. It can be seen from this figure that experimental data on the phase equilibria associated with the ε phase are rather scarce, and specifically no experimental data other than microhardness values are available for the ε/δ-Mn phase equilibrium. Moreover, the results of phase equilibria studies on the Mn–Al side of the Fe–Mn–Al system, as determined by Chakrabarti [12], are not consistent with the existing phase diagram of the Mn–Al binary system. For these reasons it was felt that the phase equilibria of the Mn-rich portion of the Mn–Al system should be re-examined.

The specific purpose of the present study was to establish the phase equilibria connected with the ε phase in the Mn-rich part of the Mn–Al system. In previous investigations the phase equilibria of the Mn–Al system were mainly determined by methods such as thermal analysis, specific heat measurements, and metallography, in which alloy compositions were kept constant and temperatures were changed [1–8], whereas, in this study, the phase equilibria have been determined over a wider composition range using the

* Corresponding author.

SSDI 0925-8388(95)02144-2

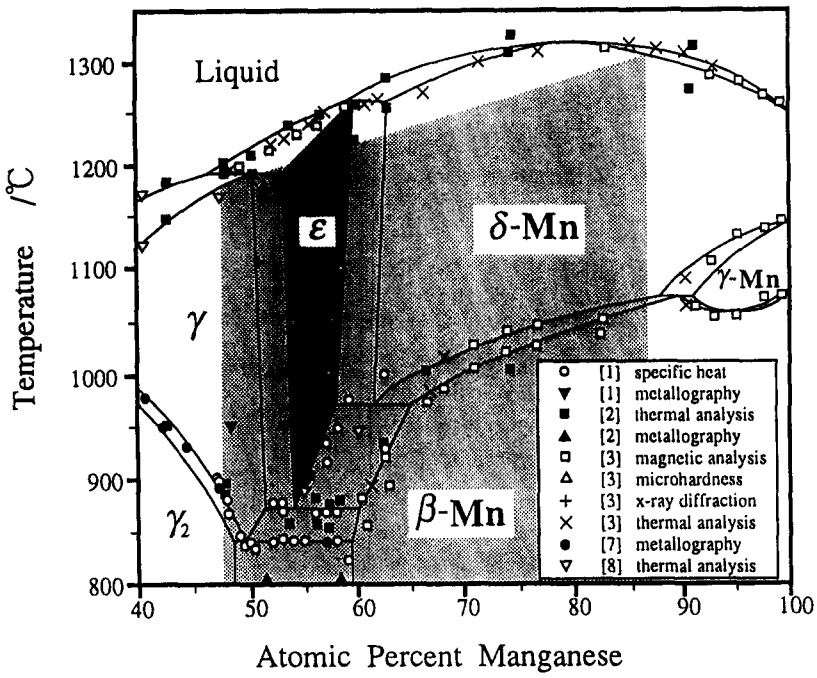

Fig. 1. Mn-rich portion of the Mn–Al phase diagram as assessed by McAlister and Murray [9]. The shaded part is the region studied in the present work.

diffusion couple technique in which the temperature is fixed. Other techniques like metallography, X-ray diffraction (XRD), differential scanning calorimetry (DSC), and transmission electron microscopy (TEM) have been utilised to confirm the results obtained by the diffusion couple technique.

2. Experimental procedure

Binary Mn–Al alloys were made in alumina crucibles by melting electrolytic manganese (99.9% pure) and aluminium (99.99% pure) in a high frequency induction furnace under an argon atmosphere. The compositions of the alloys so made and used in this study are presented in Table 1.

The alloy buttons were cut into small pieces and sealed in argon-filled quartz capsules for equilibration treatments in the temperature range 800–1200 °C; they were then used to make specimens for metallographic examination and microanalysis by energy dispersion spectroscopy (EDS). Alcoholic 20% HNO_3 solution was used as the etchant for metallographic examination.

Since some of the Mn–Al alloys were too brittle to lend themselves to the preparation of solid/solid diffusion couples, the solid/gas diffusion couple method, which has been used to determine the phase equilibria in the Fe–Mn–Al system [13], was adopted in this study because the high vapour pressure of Mn would ensure the establishment of equilibrium in a reasonable time interval. Solid/gas diffusion couples were made by sealing the Mn–Al specimens in transparent quartz capsules together with pure Mn and equilibrating them at 900–1100 °C for periods ranging from 240 to 24 h, depending on the temperature used.

After examining the microstructure, the concentration–penetration curves for each element were determined by EDS, and the equilibrium composition of each phase was obtained by extrapolating the curves to the phase boundaries. In addition, microhardness measurements were also performed on some of the diffusion couples.

XRD using Cu radiation and DSC were carried out to identify the phase structures and phase equilibria obtained in the diffusion couples. DSC studies were

Table 1
The chemical composition of as-cast specimens

Alloy	Composition (at.%)	
	Mn	Al
M83	83.76	16.24
M71	71.67	28.24
M67	67.25	32.75
M64	64.43	35.57
M61	61.39	38.61
M57	57.60	42.40
M55	55.89	44.11
M53*	53.5	46.5
M51	51.47	48.53
M41	41.62	58.38

* Nominal value.

conducted at heating and cooling rates of 3 °C min^{-1} or less using sintered Al_2O_3 as the reference specimen.

3. Results and discussion

3.1. Phase equilibria

It was found that the equilibrium compositions of the phases present were almost the same in all the solid/gas diffusion couples treated at the same temperature but for different times, and were in agreement with those determined from the solid/solid diffusion couples, thereby indicating that the phase boundary in all the solid/gas diffusion couples had reached local equilibrium.

The major feature of the microstructures is that there are three interphase boundaries in the case of the M51/Mn diffusion couples treated at a temperature above 900 °C (see Fig. 6). However, the concentration profiles from all the M51/Mn diffusion couples show that there exist only two phase boundaries at high temperature. A typical example of the concentration profile from the M51/Mn diffusion couple treated at 1070 °C for 72 h is given in Fig. 2. The phase boundary formed in the ε phase, and shown as a dotted line, will be discussed in detail in the next section. The results obtained from the diffusion couples indicate that the ε phase region is wider than that reported by previous workers, and extends to higher Mn contents. In order to further confirm these results, metallographic studies were carried out to determine phase equilibria. It was found that some specimens exhibited duplex microstructures as shown in Fig. 3, which is the microstructure for the M71 alloy annealed at 1050 °C for 72 h. Metallographic observations for all the alloys examined are shown in Fig. 4. The compositions of the phase boundaries determined from diffusion couple specimens and from the two-phase alloys are summarized in Table 2, from where it can be seen that a good agreement exists between the equilibrium compositions determined by both the methods. All the results on the phase equilibria obtained in the present study are plotted in the proposed phase diagram shown in Fig. 5, in which the estimated phase equilibria are indicated by dashed lines. The ε/δ-Mn (disordered b.c.c. structure) phase equilibrium exists between 68 and 74 at.% Mn, rather than between 58 and 62 at.% Mn as reported earlier. This is the largest discrepancy between the present study and previous ones. The γ (disordered b.c.c. structure)/ε phase equilibrium obtained in the present study is basically in agreement with the previous results, but shifted slightly to the Mn-rich side. The existence of the two eutectoid reactions $\varepsilon \rightarrow \gamma + \beta$-Mn and $\gamma \rightarrow \gamma_2$ (Mn_5Al_8:Cr_5Al_8 type) + β-Mn, reported to take place at 870 and 840 °C, is confirmed by means of DSC in the present study, while another eutectoid reaction δ-Mn $\rightarrow \varepsilon + \beta$-Mn, previously reported as occurring at

Fig. 3. Microstructure of the M71 alloy annealed 1050 °C for 72 h.

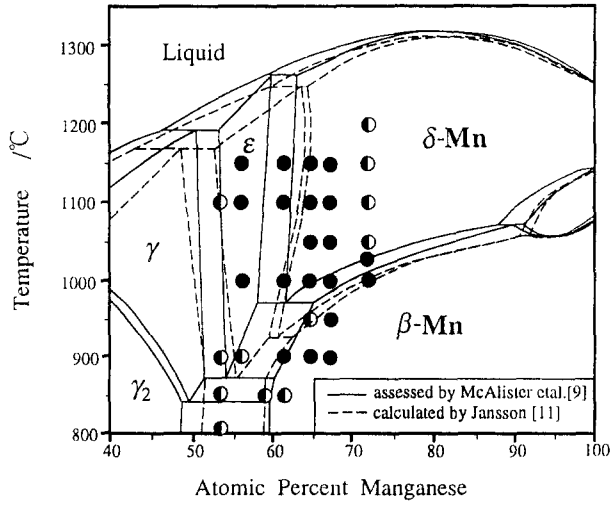

Fig. 4. Alloy specimens treated at different temperatures in this study: ●, single phase alloy; ◐, two-phase alloy.

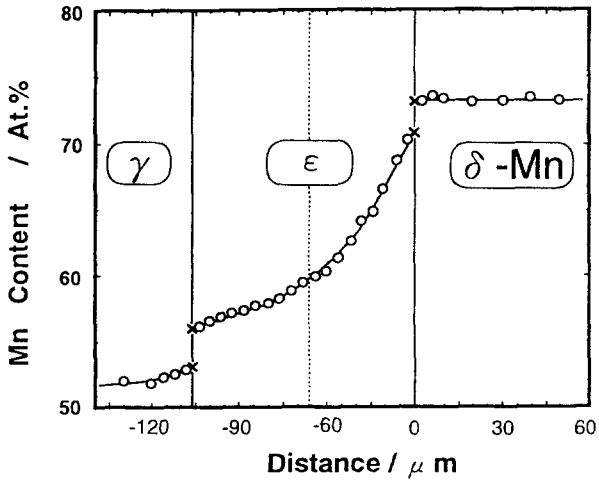

Fig. 2. Concentration profile from the M51/Mn diffusion couple annealed at 1070 °C for 72 h.

Table 2
Equilibrium composition determined in the present study

Alloy or couple	Temperature (°C)	Equilibrium composition (at.% Mn)											
		γ_2	β-Mn	γ	β-Mn	γ	ε	ε	β-Mn	ε	δ-Mn	δ-Mn	β-Mn
M71	1200	—	—	—	—	—	—	—	—	69.7	71.5	—	—
M71, M51/Mn	1150	—	—	—	—	51.6	54.4	—	—	70.3, 70.2	72.1, 72.0	—	—
M71, M51/Mn	1100	—	—	—	—	52.4	55.1	—	—	71.0, 71.0	72.5, 73.8	—	—
M51/Mn	1070	—	—	—	—	52.9	55.6	—	—	71.3	73.2	—	—
M67/Mn	1050	—	—	—	—	*	*	—	—	71.2	73.6	77.9	81.0
M67/Mn	1030	—	—	—	—	*	*	71.0	73.5	—	—	—	—
M51/Mn	1000	—	—	—	—	53.1	56.0	67.4	70.2	—	—	—	—
M51/Mn	970	—	—	—	—	52.9	56.7	65.3	67.3	—	—	—	—
M64	950	—	—	—	—	*	*	64.1	67.0	—	—	—	—
M53, M51/Mn	900	—	—	—	—	52.3, 52.7	57.4, 56.8	62.2	64.9	—	—	—	—
M53	850	—	—	52.8	60.2	—	—	—	—	—	—	—	—
M53	800	51.4	60.8	—	—	—	—	—	—	—	—	—	—

* Phase boundary not determined.

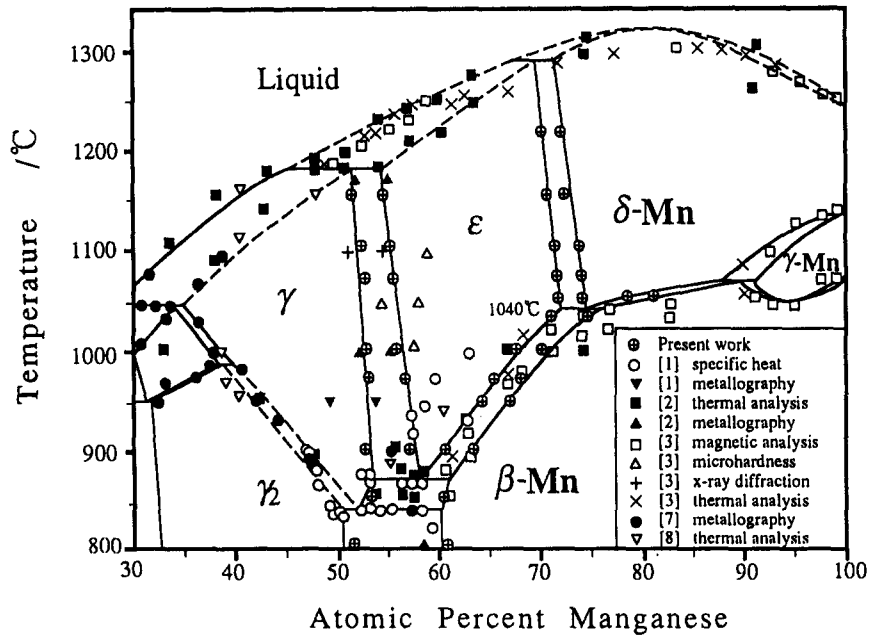

Fig. 5. Mn-rich portion of the Mn–Al binary phase diagram as determined in the present study compared with the data of previous workers.

970 °C, is found to occur at the higher temperature of 1040 °C.

It is to be expected that the shift of the ε/δ-Mn phase equilibrium will be reflected in the shape of the liquidus and solidus lines. Since both the δ-Mn and γ phases are disordered b.c.c. structures, the phase equilibrium between the liquid/δ-Mn and liquid/γ should be smoothly continuous through the compositional range of liquid/ε phase equilibrium. Applying this criterion, the loci of the liquidus and solidus lines (dashed lines in Fig. 5), have been estimated by combining the phase rule and the data from the present and previous studies.

3.2. Phase transformation of the ε phase

As mentioned earlier, three phase boundaries were observed by optical microscopy in all M51/Mn diffusion couples. Fig. 6 shows the microstructure and concentration profile observed in the M51/Mn diffusion couple annealed at 1100 °C for 24 h. It can clearly be seen that there is no concentration gap at the slightly non – planar middle phase boundary. Fig. 7 shows the two X-ray patterns from the alloys M55 and M61 quenched from 1100 °C. The concentration profiles from the diffusion couples connected with these two alloys annealed at high temperature indicate the presence of the same ε phase. It is clear from the XRD and EDS results that, on quenching the original high temperature ε phase structure is retained in the M55 alloy, whereas the same ε phase transforms to the β-Mn structure in the M61 alloy. Further XRD examinations on some other alloys show that the ε phase with more than 58 at.% Mn transforms to the β-Mn phase, which is in good agreement, as shown in Fig. 6, with the composition at the phase boundary formed in

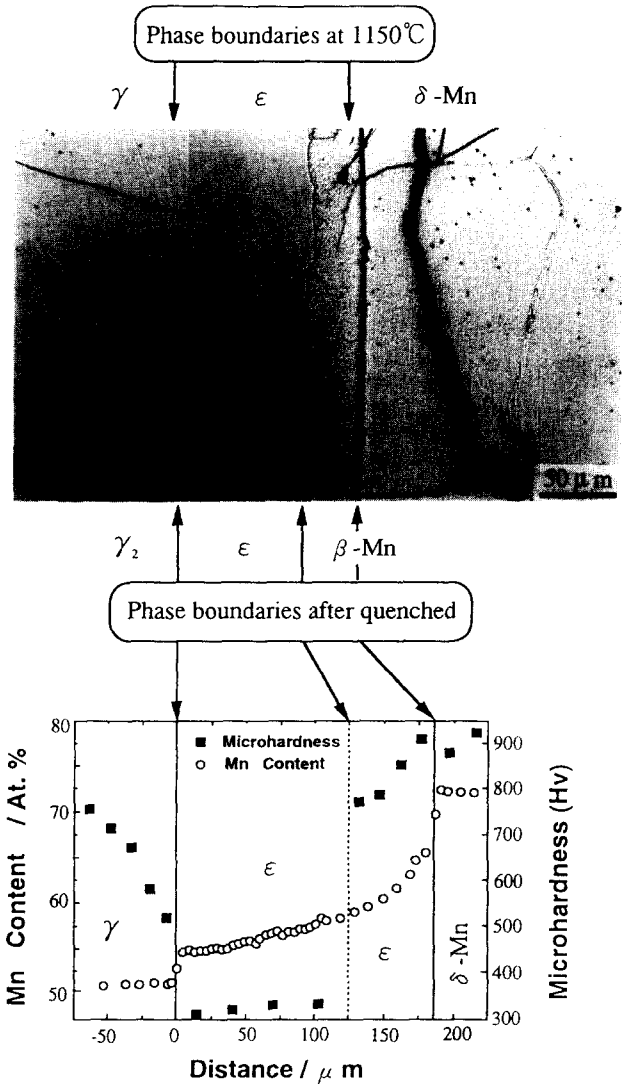

Fig. 6. Microstructure, concentration profile and microhardness measurement taken on the M51/Mn diffusion couple annealed at 1150 °C for 24 h.

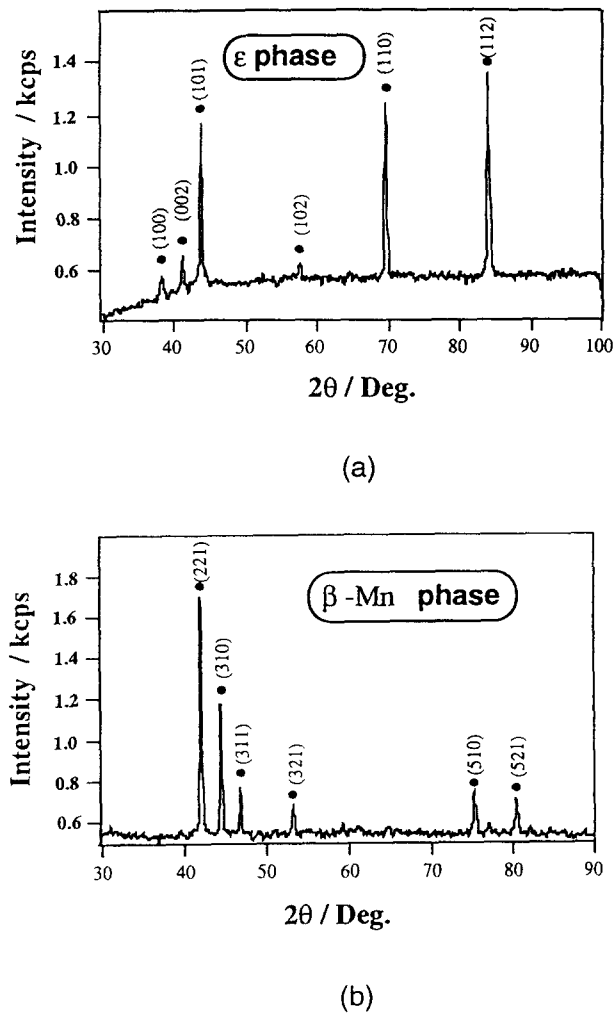

Fig. 7. X-ray patterns from the (a) M55 and (b) M61 alloys quenched from 1100°C.

the ε phase. It is also confirmed by XRD that the δ-Mn phase at high temperature transforms to the β-Mn structure on quenching. The microhardness results obtained from the diffusion couple specimen shown in Fig. 6 clearly delineate the existence of a microhardness gap at the three phase boundaries. It is obvious that the alloy hardness in the composition range 58 to around 73 at.% Mn is due to the formation of the β-Mn phase on cooling. From these observations it is thus surmised that the middle phase boundary, at which there is no concentration gap, is formed during quenching. It is worthwhile noting here that the location by Koster and Wachtel [3] of the $\varepsilon/\varepsilon + \delta$–Mn phase boundary at 58 at.% Mn was based on microhardness examinations on quenched samples.

Fig. 8 shows the phase stability range of the ε phase on quenching and includes the $T_0^{\varepsilon/\beta Mn}$ temperature vs. composition line at which the chemical free energy of the ε phase is equal to that of the β-Mn phase. The

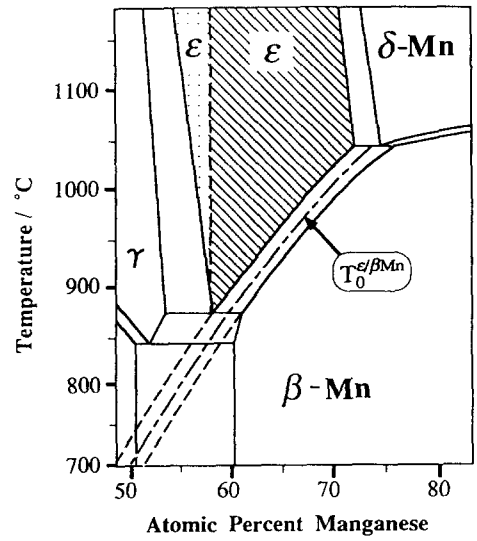

Fig. 8. Phase transformation of the ε phase. The alloys of shaded area transform from ε to β-Mn phase on quenching.

$T_0^{\varepsilon/\beta Mn}$ temperature for the 58 at.% Mn alloy is about 850 °C, which means that the driving force for the formation of the β-Mn phase from the ε phase is large and negative at low temperatures. This indicates that a massive or martensitic transformation invariant composition may occur at any temperature sufficiently below $T_0^{\varepsilon/\beta Mn}$. Furthermore, the phase equilibria associated with the ε phase, which decomposes through a eutectoid reaction, are very similar to that of the V-shaped b.c.c. β phase of the Cu–Ga, Cu–Zn, Cu–Al, Ag–Cd, Ag–Al and Ag–Zn systems, which exhibits a massive transformation [14]. Since the β-Mn phase is formed and developed from the original ε/β-Mn interphase boundary on quenching from the ε phase, as shown in Fig. 6, it is evident that there exists a distinct possibility that an $\varepsilon \rightarrow \beta$-Mn massive transformation can occur on quenching. The discrepancy between the present study and previous data regarding the ε phase field can thus be explained as due to the structural transformation of the ε phase during cooling, which has not been taken into account in earlier studies.

4. Conclusions

(i) The phase equilibria in the composition range 50 to around 80 at.% Mn in the Mn–Al system were determined. It is shown that the ε/δ-Mn phase region is wider than that reported before, and the phase boundary is at about 72 at.% Mn rather than at 60 at.% Mn.

(ii) The eutectoid reaction $\delta\text{-Mn} \rightarrow \varepsilon + \beta\text{-Mn}$ occurs at 1040 °C, but not at about 970 °C.

(iii) The ε phase with more than 58 at.% Mn content transforms to the β-Mn phase, while the same phase with less than 58 at.% Mn retains the high temperature phase structure on quenching.

Acknowledgements

The authors would like to thank Mr. M. Ise for his help in carrying out this work and Dr. L Chandrasekaran of DRA Farnborough, UK for help in preparation of the manuscript for publication.

References

[1] H. Kono, *J. Phys. Soc. Jpn.*, *13* (1958) 1444.
[2] A.J.J. Koch, P. Hokkeling, M.G.v.d. Steeg and K.J. DeVos, *J. Appl. Phys.*, *31* (1960) 75.
[3] W. Koster and E. Wachtel, *Z. Metallkd.*, *51* (1960) 271.
[4] L.M. Magat, Ya.S. Shur, G.S.Kandaurova, G.M. Makarova and N.I. Guselnikova, *Fiz. Met. Metalloved.*, *23* (1967) 226.
[5] H.W.L. Phillips, *J. Inst. Met.*, *69* (1943) 275.
[6] M.A. Taylor, *Acta Metall.*, *8* (1960) 256.
[7] T. Godecke and W. Koster, *Z. Metallkd.*, *62* (1971) 727.
[8] J.L. Murray, A.J. McAllister, R.J. Schaefer, L.A. Bendersky, F. Biancaniello and D.L. Moffat, *Metall. Trans.*, *18A* (1987) 385.
[9] A.J. McAllister and J.L. Murray. *Bull. Alloy Phase Diagr.*, *8* (1987) 438.
[10] M. Ellner, *Metall. Trans.*, *21A* (1990) 1669.
[11] A. Jansson, *Metall. Trans.*, *23A* (1992) 2953.
[12] D.J. Chakrabarti, *Metall. Trans.*, *8B* (1977) 121.
[13] X.J. Liu and S.M. Hao, *Scripta Metall. Mater.*, *28* (1993) 611.
[14] T.B. Massalski, *Phase Transformations*, ASM, 1970, p. 433.